

LAST LAYER MARGINAL LIKELIHOOD FOR INVARIANCE LEARNING

POLA SCHWÖBEL,
MARTIN JØRGENSEN,
SEBASTIAN W. OBER, AND
MARK VAN DER WILK

ABSTRACT. Data augmentation is often used to incorporate inductive biases into models. Traditionally, these are hand-crafted and tuned with cross validation. The Bayesian paradigm for model selection provides a path towards end-to-end learning of invariances using only the training data, by optimising the marginal likelihood. We work towards bringing this approach to neural networks by using an architecture with a Gaussian process in the last layer, a model for which the marginal likelihood can be computed. Experimentally, we improve performance by learning appropriate invariances in standard benchmarks, the low data regime and in a medical imaging task. Optimisation challenges for *invariant* Deep Kernel Gaussian processes are identified, and a systematic analysis is presented to arrive at a robust training scheme. We introduce a new lower bound to the marginal likelihood, which allows us to perform inference for a larger class of likelihood functions than before, thereby overcoming some of the training challenges that existed with previous approaches.

1. INTRODUCTION

Human learners generalise from example to category with seemingly little effort. In this paper, we aim to imitate such inductive behaviour in machine learning models. Based on finitely many examples, statistical models make predictions on unseen data points in a high-dimensional space. This generalisation is enabled by *inductive biases*. In *Steps toward Artificial Intelligence* Marvin Minsky [1961] highlights the importance of one specific inductive bias:

‘One of the prime requirements of a good property is that it be invariant under the commonly encountered equivalence transformations. Thus for visual Pattern-Recognition we would usually want the object identification to be independent of uniform changes in size and position.’

In modern machine learning pipelines invariances are achieved through data augmentation. If we, for example, would like our neural network to be invariant w.r.t. rotation, we simply present it with rotated versions of the input data. Data augmentation schemes are almost always hand-crafted, based on assumptions about the data, or found by cross validation. This work aims to learn invariances with

Pola Schwöbel, Technical University of Denmark, posc@dtu.dk.

Martin Jørgensen, University of Oxford, martinj@robots.ox.ac.uk.

Sebastian W. Ober, University of Cambridge, swo25@cam.ac.uk.

Mark van der Wilk, Imperial College London, m.vdwilk@imperial.ac.uk.

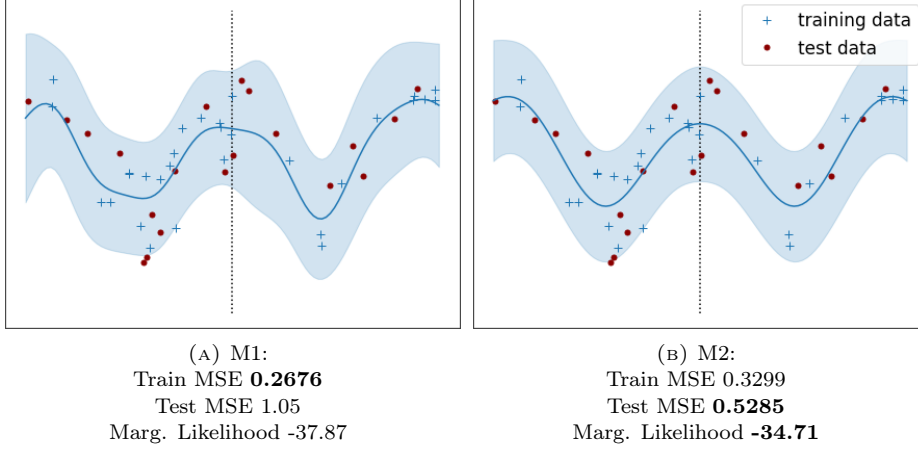


FIGURE 1. The non-invariant M1 has higher a likelihood, but the invariant M2 generalises better (lower test MSE). The marginal log-likelihood correctly identifies M2 as better.

back-propagation, reducing the need for human intervention in the design of ML algorithms.

Learning invariances through gradients requires a suitable loss function. Standard neural network losses like negative log-likelihood or mean squared error, however, solely describe how tightly we fit the training data. Good inductive biases (e.g. convolutions, l_2 -regularisation) constrain the expressiveness of a model, trading a potentially *worse* fit on the training data for better generalisation performance. Thus, they can not be learned by minimising the training loss alone.

In opposition to standard training losses, the *marginal likelihood* for a model parametrised by weights w , data y and hyperparameters θ

$$p(y|\theta) = \int p(y|w)p(w|\theta)dw, \quad (1.1)$$

correlates with generalisation and provides a general way, independent of parametrisation, to perform model comparison [Williams and Rasmussen, 2006, Rasmussen and Ghahramani, 2001, MacKay, 2002]. If employed in neural networks the marginal likelihood would present a powerful objective.

Van der Wilk et al. [2018] showed that for the Gaussian process case, where the marginal likelihood is analytically tractable, it can indeed be used to learn invariant representations. While the marginal likelihood is intractable for an entire neural network, it can be computed if we only perform inference on the last layer. Wilson et al. [2016a] have had recent success with this – can their strategy for estimating marginal likelihoods in deep neural networks be applied for learning inductive biases in such models? In order to investigate this, ultimately arriving at an algorithm for invariance learning in deep neural networks, we will proceed as follows:

- (1) Construct a suitable model allowing for marginal likelihood computation and thus invariance learning: Inspired by Deep Kernel learning, we opt for

a Bayesian last layer model, combining a neural network with a Gaussian Process layer.

- (2) Investigate strengths and weaknesses: We successfully apply the approach experimentally but note that learning inductive biases does not work *out of the box*. We provide a detailed discussion on training procedures for inference.
- (3) Overcome challenges: We derive a new variational bound which effectuates sampling Gaussian processes by Matheron’s rule [Wilson et al., 2020] in order to perform inference for non-Gaussian likelihoods, alleviating some of the discussed problems.

2. RELATED WORK

Bayesian Deep Learning aims to provide principled uncertainty quantification for deep models. Exact computation for Bayesian deep models is intractable, so different approximations have been suggested. Variational strategies [Blundell et al., 2015] maximise the evidence lower bound (ELBO) to the marginal likelihood, thereby minimising the gap between approximate and true posteriors. In order to remain computationally feasible, approximations for Bayesian neural networks are often crude, and while the weight posteriors are useful in practice, the marginal likelihood estimates are typically imprecise, which can introduce bias in hyperparameter estimation [Blundell et al., 2015, Turner and Sahani, 2011]. Hyperparameter estimation in deep Gaussian processes has achieved more success [Damianou and Lawrence, 2013, Dutordoir et al., 2020], but training deep Gaussian processes can be challenging. Some very recent works have shown initial promise in using the marginal likelihood for hyperparameter selection in Bayesian neural networks [Ober and Aitchison, 2020, Immer et al., 2021, Dutordoir et al., 2021], and may be useful in the future.

Deep Kernel Learning (DKL; Hinton and Salakhutdinov [2007], Calandra et al. [2016], Bradshaw et al. [2017]) trades a rough approximation of all weights for a tight approximation to the last-layer posterior. The last layer is replaced with a Gaussian process, where marginal likelihood estimation is known to be accurate [Burt et al., 2020]. In particular, Wilson et al. [2016a,b] had significant recent success, achieving improved uncertainty estimates. Their results indicate such a neural network-GP hybrid is a promising candidate for invariance learning. Ober et al. [2021] argue that there can be difficulties with overfitting in DKL models, but they also show that overfitting can be mitigated. We discuss these issues in more depth as we describe our training procedure.

Data Augmentation is traditionally used to incorporate invariances into deep learning models. Where good invariance assumptions are available a priori (e.g. for natural images) the approach often improves generalisation performance and is ubiquitous in deep learning pipelines. Instead of relying on assumptions about the data and hand-crafting, recent approaches *learn* data augmentation schemes. Cubuk et al. [2020, 2019] and Ho et al. [2019] use grid searches on validation data, reinforcement learning and evolutionary search, respectively. Hauberg et al. [2016] employ an unsupervised approach. Similar to our work, Benton et al. [2020] learn data augmentations on training data end-to-end. Instead of using the marginal likelihood as an objective function, they add a regularisation term to the negative log-likelihood loss that explicitly enforces invariance. Choosing the magnitude of

this regularisation term via cross-validation can be avoided, since the loss function is relatively flat. However, the method relies on an explicit formulation of this regularisation, and thus on an understanding of the parameters in question. We instead learn invariances via the marginal likelihood, which only depends on the effect of the parameters and is independent of the specific parameterisation. This makes the marginal likelihood a promising avenue for future work, which may want to incorporate invariances whose parameterisations are harder to interpret.

3. BACKGROUND

3.1. Gaussian processes. A Gaussian process (GP) [Williams and Rasmussen, 2006] is a distribution on functions with the property that any vector of function values $\mathbf{f} = (f(x_1), \dots, f(x_N))$ is Gaussian distributed. We assume zero mean functions and real valued vector inputs, i.e. $x_i \in \mathbb{R}^d$. In this case, the distribution of an arbitrary set of evaluations is given by $\mathcal{N}(0, \mathbf{K})$ with $[\mathbf{K}]_{ij} = k(x_i, x_j)$.

After observing function values \mathbf{f} , the predictive distribution at a test set is still a tractable Gaussian. However, computing it requires inverting \mathbf{K} at a cost above quadratic, which becomes infeasible for large datasets. Sparse variational GP approximations [Titsias, 2009, Hensman et al., 2013] overcome this by introducing a tractable approximate posterior Gaussian process. This is created by conditioning the prior on M inducing variables $\mathbf{u} \in \mathbb{R}^M$, and specifying their marginal distribution with $q(\mathbf{u}) = \mathcal{N}(\mathbf{m}, \mathbf{S})$ (for overviews see [Bui et al., 2017, van der Wilk et al., 2020]). This results in a variational predictive distribution [Hensman et al., 2013]

$$q(f(x^*)) = \mathcal{N}(\boldsymbol{\alpha}(x^*)^\top \mathbf{m}, k(x^*, x^*) - \boldsymbol{\alpha}(x^*)^\top (\mathbf{K}_{zz} - \mathbf{S}) \boldsymbol{\alpha}(x^*)), \quad (3.1)$$

where \mathbf{z} is inducing *locations*, \mathbf{K}_{zz} is the matrix with entries $k(z_i, z_j)$, and $\boldsymbol{\alpha}(x^*) = \mathbf{K}_{zz}^{-1} k(\mathbf{z}, x^*)$. The resulting evidence lower bound (ELBO) is given by

$$\log p(y) \geq \sum_{n=1}^N \mathbb{E}_{q(f_n)} [\log p(y_n | f_n)] - \text{KL}[q(\mathbf{u}) || p(\mathbf{u})], \quad (3.2)$$

where $p(\mathbf{u}) = \mathcal{N}(0, \mathbf{K}_{zz})$. Maximising this bound minimises the KL divergence between our approximation and the true posterior [Matthews et al., 2016].

3.2. Construction and Inference in Invariant Gaussian Processes. A function $f : \mathcal{X} \rightarrow \mathcal{Y}$ is said to be *invariant* w.r.t. a transformation $t : \mathcal{X} \rightarrow \mathcal{X}$ if

$$f(x) = f(t(x)) \quad \forall x \in \mathcal{X} \quad \forall t \in \mathcal{T}. \quad (3.3)$$

In words, an invariant function will have the same output for a certain range of inputs. We will refer to such ranges of inputs as *orbits*. A straightforward way to construct invariant functions, assuming finitely many elements in \mathcal{T} , is to simply sum over the set of transformations. This construction extends to the *continuous* case, where we replace the orbit \mathcal{T} with an augmentation distribution $p(x_a | x)$. That is, f can be constructed as

$$f(x) = \sum_{t \in \mathcal{T}} g(t(x)), \quad \text{or} \quad f(x) = \int g(x_a) p(x_a | x) dx_a. \quad (3.4)$$

Van der Wilk et al. [2018] exploit this construction to build an invariant GP: they place a GP prior on $g \sim \mathcal{GP}(0, k_g(\cdot, \cdot))$. Since Gaussians are closed under

summations f is a Gaussian process too. By construction f is invariant to the augmentation distribution $p(x_a|\cdot)$ and its kernel is given by

$$k_f(x, x') = \iint k_g(x_a, x'_a) p(x_a|x) p(x'_a|x') dx_a dx'_a. \quad (3.5)$$

For standard variational inference the first term of the ELBO, $\mathbb{E}_{q(f_n)} [\log p(y|f_n)]$, is not analytically tractable in all cases. For the Gaussian likelihood, a closed form solution is available, however, this is no longer trivial for the invariant construction. We can note $\mathbb{E}_{q(f(x))} \log p(y|f(x)) = \mathbb{E}_{q(f(x))} \log \mathcal{N}(y; f(x), \sigma^2)$, where $q(f)$ is Gaussian with mean μ and variance τ . On this inspection, the variational expected log-likelihood is given by

$$\mathbb{E}_{q(f_n)} [\log p(y_n|f_n)] = -\log 2\pi\sigma^2 - \frac{1}{2\pi} (y^2 - 2y_n\mu + \mu^2 + \tau), \quad (3.6)$$

hence, analytically available when knowing μ and τ . However, this is not the case for an invariant GP f , since we can not compute the integral defining f . [Van der Wilk et al. \[2018\]](#) overcame this obstacle by estimating μ and τ under the double-sum kernel formulation. For example, an unbiased estimator $\hat{\mu}$ for μ is given by

$$\hat{\mu} := \sum_{x_a \sim p(x_a|x)} k_g(x_a, \mathbf{z}) \mathbf{K}_{\mathbf{z}\mathbf{z}}^{-1} \mathbf{m}, \quad (3.7)$$

i.e. an estimator based on samples from the orbit distribution $p(x_a|x)$. This originates from an *inter-domain* formulation, i.e. $k_f(z, x) = \int k_g(z, x_a) p(x_a|x) dx_a$. Similarly, they present an unbiased estimator for τ , and we refer the reader to their paper for an expression for this.

3.3. Image transformations. In machine learning, we typically specify a family of functions and aim to infer the parameters. In the framework of [Van der Wilk et al. \[2018\]](#), possible invariances are parameterised through the augmentation distribution $p(x_a|x)$. While the framework is general and can be applied to any reparameterisable augmentation distribution, we focus on learning the correct distribution on affine transformations, as is done in similar work [[Benton et al., 2020](#)].

To transform an image, we apply a transformation t_ϕ to a coordinate grid which interpolates the input image x to generate the transformed image x_a .¹ The transformation is controlled by $\phi = (\alpha, s^x, s^y, p^x, p^y, t^x, t^y)$, which describes rotation, scale, shearing and horizontal and vertical translation and is sampled from a uniform distribution $\phi \sim U(-\phi_{\min}, \phi_{\max})$. The invariance is controlled by adjusting the vectors of ϕ_{\min}, ϕ_{\max} . Which transformations will be used, and to what extent, will be learned based on the specific training set. We wish to stress that generating the orbit distributions is not restricted to affine image transformation, in fact, when using the marginal likelihood as an objective we are *independent of parametrisation*. This stands out from the approach introduced by [Benton et al. \[2020\]](#) where the regularisation must be interpretable. The next sections show how these principles have potential even in neural network models, beyond the single layer GPs of [van der Wilk et al. \[2018\]](#).

4. MODEL

As discussed in Sec. 1, we harness the marginal likelihood as the objective function for learning invariances. Computing this quantity requires evaluating integrals of

¹Code from github.com/kevinzakka/spatial-transformer-network after [Jaderberg et al. \[2015\]](#).

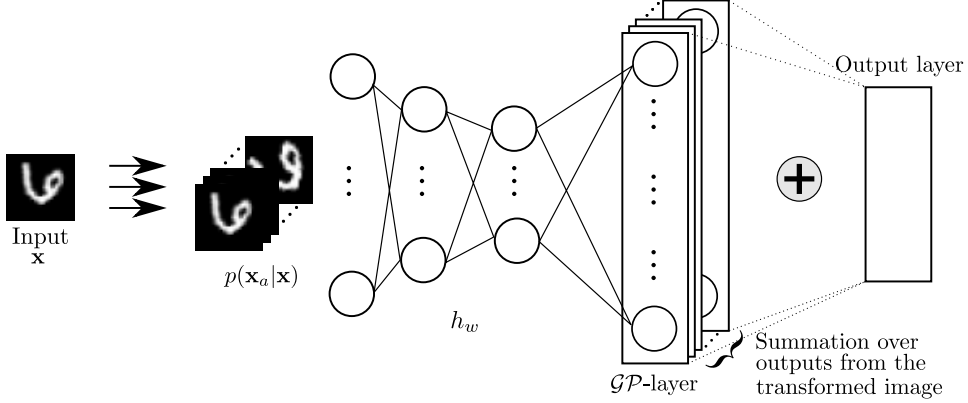


FIGURE 2. A visualisation of the model pipeline. For any input x , we sample from the orbit distribution $p(x_a|x)$; each of these sample is passed through a neural network parametrised by w . The last layer is a GP, on which we sum across sample outputs to create an invariant function.

the form (1.1) which are intractable for complex models such as neural networks. For Gaussian processes, however, inference is routinely performed, e.g. by choosing a Gaussian likelihood such that (1.1) has a closed form. We thus choose a Deep Kernel Learning architecture combining a neural network for performance with a Gaussian process layer for estimating the marginal likelihood. See Fig. 2 for a graphical representation.

Deep Kernels take advantage of the fact that covariance functions are closed under well-defined transformations of their input. That is, if $k_g(\cdot, \cdot)$ is a covariance function on $\mathbb{R}^D \times \mathbb{R}^D$, then $k_g(h_w(\cdot), h_w(\cdot))$ is a covariance function on $\mathbb{R}^d \times \mathbb{R}^d$ for mappings $h_w : \mathbb{R}^d \rightarrow \mathbb{R}^D$.

In our case, h_w is a neural network parametrised by weights w , and hence w are viewed as hyperparameters of the kernel. The Gaussian process prior becomes

$$p(g) = \mathcal{GP}(0, k_g(h_w(\cdot), h_w(\cdot))). \quad (4.1)$$

The idea is to learn w along with the kernel hyperparameters. Importantly, this model remains a GP and so standard GP inference as described in Section 3 applies.

Our invariant model is constructed by applying a deep kernel to the invariant formulation from (3.4):

$$f(x) = \int g(h_w(x_a)) p(x_a|x, \phi) dx_a. \quad (4.2)$$

Here g is a GP with prior as given in (4.1) and h_w is a domain-specific neural network. Thus, combining (3.5) and (4.2), f is an *invariant* GP with a *deep* kernel given as

$$k_f(x, x') = \int k_g(h_w(x_a), h_w(x'_a)) p(x_a|x) p(x'_a|x') dx_a dx'_a. \quad (4.3)$$

The model is trained to fit observations y through the likelihood function $y \sim p(y|f(x))$, where we assume observations y_i are independent conditioned on the marginals $f(x_i)$. The invariant GP training objective for Gaussian likelihoods [van der Wilk et al., 2018] remains unchanged when using the deep kernel. However,

as we will discuss, several issues prevent the standard training procedures [Wilson et al., 2016a,b] from working. In the next sections we investigate why, provide solutions, and introduce a new ELBO that is suitable for more general likelihoods which further improves training behaviour. We refer to our model as the *invariant Deep Kernel GP (InvDKGP)*.

5. EXPERIMENTS: DEEP KERNEL INVARIANCE LEARNING WITH GAUSSIAN LIKELIHOOD

5.1. Preliminaries. Is the marginal likelihood really necessary? Section 1 motivated the marginal likelihood for invariance learning. We justify this choice experimentally by attempting to train invariances using a standard neural network with maximum likelihood loss. Fig. 3 shows invariances learned on rotated MNIST (rotMNIST, see Sec. 7.1 for a description of the dataset) by using a neural network and maximum likelihood loss for two different initialisations (blue, green), which indeed collapse as suggested by the theory. The marginal likelihood solution (red) instead identifies appropriate invariances.

Coordinate ascent training: The promise of deep kernel learning lies in training the neural network and GP hyperparameters *jointly*. However, prior works have noted the shortcomings of this approach [Ober et al., 2021, Bradshaw et al., 2017]: The DKL marginal likelihood correctly penalises complexity for the last layer only, while the neural network hyperparameters are not guarded from overfitting. In our setting, joint training produces overfit weights, correlating all training points independent of orientation, causing a loss of signal for the invariance parameters (see Fig. 4). For invariance learning, we thus pre-train the neural network using negative log-likelihood loss, then replace the fully connected last layer. We fix the neural network weights, as the marginal likelihood is a good objective given fixed weights (we recover the standard GP setting on a transformed input space in this case). However, some adaptation of the neural network is beneficial. We thus continue training with coordinate-ascent training scheme: iterating between updating the neural network, and the GP variational parameters and orbit parameters.

Training scheme: Exploiting the ideas from above, we start by training simple convolutional neural networks (CNNs, see Appendix for details). After pre-training the CNN, we replace the last fully connected layer with a GP and continue training. In the non-invariant case we train all parameters jointly from here. When learning invariances, we iterate between updating the GP variational- and hyperparameters, and the neural network weights. We initialise inducing points using the “greedy variance” method suggested by Burt et al. [2020], see Appendix for all other hyper-, variational and optimisation parameter settings. This training scheme is used in all following experiments.

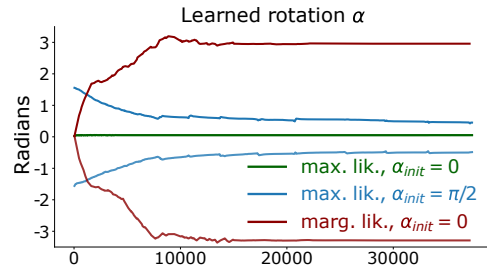


FIGURE 3. Max. likelihood (green, blue, *collapsing*) and marg. likelihood (red, *useful*) invariances.

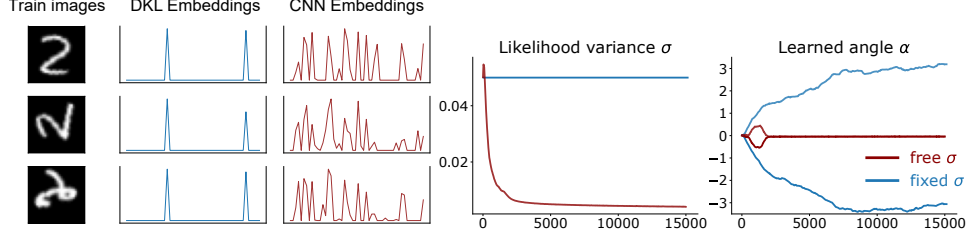


FIGURE 4. *Left:* Training images with different orientations and their embeddings. Embeddings produced by joint Deep Kernel Learning (DKL, middle column) are similar for all inputs: little improvement can be gained on the training data by being rotationally invariant. CNN embeddings on the right differ depending on input orientation – signal to learn $p(x_a|x)$ from. *Right:* Runs with fixed (red) and non-fixed (blue) kernel and likelihood variance on rotMNIST. The augmentation distribution collapses for non-fixed variances.

5.2. MNIST subsets – the low data regime. The generalisation problem is particularly difficult when training data is scarce. In such cases, inductive biases are especially important and usually parameter-rich neural networks rely on heavy data augmentation when applied to smaller data sets. We train on different subsets of MNIST [LeCun et al., 2010]. The invariant models outperform both CNNs and non-invariant deep kernel GPs. The margin is larger the smaller the training set — with only 1250 training examples we can nearly match the performance of a CNN trained on full MNIST. We conclude it is possible to learn useful invariances even from small data. This data efficiency is desirable since models trained on small datasets benefit crucially from augmentation as can be seen in Fig. 5.

Likelihood misspecification: We have, unnaturally for a classification task, used the Gaussian likelihood in Sec. 5.2 due to its closed-form ELBO. In the Gaussian case, the penalty for not fitting the correct label value becomes large and we can therefore overfit the training data. To alleviate this problem, we had to manually tune and fix likelihood and kernel variance (see Fig. 4, right). To remove this manual tuning, we derive an ELBO that works with likelihoods like softmax. This broadens model specification, but additionally increases convergence speed by a factor of 2.

6. A SAMPLE BASED BOUND FOR LOG-CONCAVE LIKELIHOODS

The key observation for inference in the Gaussian likelihood case was *unbiasedness* of the estimators. In this section, we introduce a controlled bias to allow for easy inference in a wide class of likelihood models. In the limit of infinite sampling, the bias disappears and the invariance doesn't add any additional approximation error.

Recall that $f(x)$ constructed in (3.4) is intractable but can be estimated by Monte Carlo sampling

$$\hat{f}(x) := \frac{1}{S_o} \sum_{i=1}^{S_o} g(x_a^i), \quad (6.1)$$

where $x_a^i \sim p(x_a|x)$. Notice,

$$f(x) = \mathbb{E}_{\prod_{i=1}^{S_o} p(x_a^i|x)} [\hat{f}(x)] =: \tilde{\mathbb{E}} [\hat{f}(x)], \quad (6.2)$$

Algorithm 1: InvDKGP forward pass	
1.	Draw S samples from the augmentation distribution $x_a^i \sim p(x_a x)$, $i = 1 \dots S$.
2.	Pass the x_a^i through the neural net h_w .
3.	Map extracted features using the non-inv. g .
4.	Aggregate samples to obtain inv. $f(x)$ by either
(i)	using the unbiased estimators in the Gaussian case, see (3.7), or,
(ii)	averaging predictions $g(h_w(x_a^i))$, $i = 1, \dots, S$ directly in the Softmax case, see (6.5).

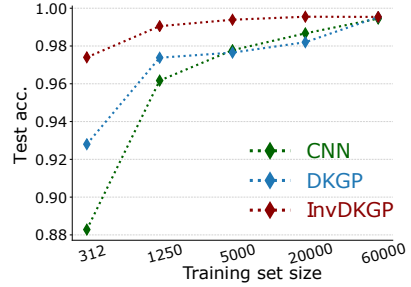


FIGURE 5. *Left:* Forward pass through the invariant Deep Kernel GP model, as outlined in Fig. 2. *Right:* Test accuracies against the training set size on MNIST. We see the invariant model (in red) generalises significantly better, especially for small training sets.

where $\prod_{i=1}^{S_o} p(x_a^i|x)$ is the product density over S_o orbit densities. Further, we remark that f is deterministic in x but stochastic in g , which is a GP. Thus, we can write

$$\mathbb{E}_{q(f(x))}[\log p(y|f(x))] = \mathbb{E}_{q(g)}[\log p(y|f(x))] \quad (6.3)$$

$$= \mathbb{E}_{q(g)} \left[\log p \left(y | \tilde{\mathbb{E}}[\hat{f}(x)] \right) \right] \geq \mathbb{E}_{q(g)} \left[\tilde{\mathbb{E}} \left[\log p \left(y | \hat{f}(x) \right) \right] \right]. \quad (6.4)$$

The last inequality is due to Jensen's inequality when we assume $\log p(y|f)$ is concave in f , i.e. the likelihood is *log-concave* in f . This is true for many common likelihoods, e.g. Gaussian and multinomial (also known as the Softmax).

Notice equality holds above when $\text{Var}(\hat{f}(x)) = 0$. This implies the bound above becomes tighter as S_o increases, hence aggressive sampling recovers accurate

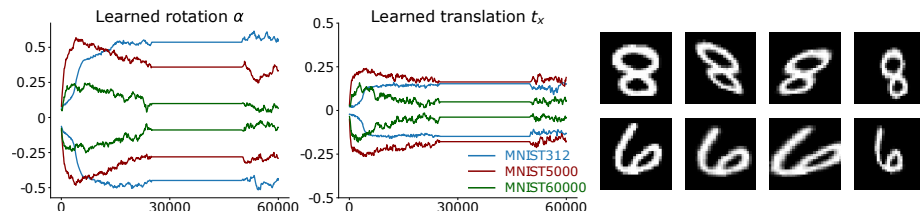


FIGURE 6. *Left:* Learned invariance parameters (rotation α in radians and x-translation t_x) for a small, medium and large dataset. We learn larger α for the smaller subsets where data augmentation is more beneficial. *Right:* Two training images x (first column) and samples from $p(x_a|x)$ (following columns) learned by the InvDKGP on MNIST with only 312 images in the training set.

	Model	Likelihood	Test acc.
M1	CNN	Softmax	0.9433
M2	Non-inv. Shallow GP	Gaussian	0.8357
M3	Non-inv. Shallow. GP	Softmax	0.7918
M4	Inv. Shallow GP	Gaussian	0.9516
M5	Inv. Shallow. GP	Softmax	0.9316
M6	Non-inv. Deep Kernel GP	Gaussian	0.9387
M7	Non-inv. Deep Kernel GP	Softmax	0.9351
M8	Inv. Deep Kernel GP	Gaussian	0.9896
M9	Inv. Deep Kernel GP	Softmax	0.9867

TABLE 1. Test accuracies on rotated MNIST. Invariant models outperform their non-invariant counterparts by far, so do deep kernels contra shallow ones. The invariant deep kernel GPs perform best, slightly outperforming state-of-the-art of 0.989 for learned invariance [Benton et al., 2020]

variational inference. The right-hand side of (6.4) can now, in an *unbiased* manner, be estimated by

$$\frac{1}{S_g} \sum_{k=1}^{S_g} \frac{1}{S_{\mathcal{A}}} \sum_{j=1}^{S_{\mathcal{A}}} \log p \left(y \middle| \frac{1}{S_o} \sum_{i=1}^{S_o} g_k(x_a^{ji}) \right). \quad (6.5)$$

Since extensive sampling is required to keep the bound above tight, it is worthwhile to consider how to efficiently perform this. From a GP perspective this is handled with little effort by sampling the approximate posteriors $q(g)$ using Matheron's rule [Wilson et al., 2020]. Thus, sampling S_g GPs is undemanding compared to sampling from the orbit. $S_{\mathcal{A}}$ denotes the number of \hat{f} samples, this can be fixed to 1 as long as S_o is sufficiently large.

Summarising this section, we have shown how we can infer through the marginal likelihood, for the wide class of log-concave likelihoods, by maximising the stochastic ELBO:

$$\frac{1}{S_g} \sum_{k=1}^{S_g} \frac{1}{S_{\mathcal{A}}} \sum_{j=1}^{S_{\mathcal{A}}} [\log p(y \mid \frac{1}{S_o} \sum_{i=1}^{S_o} g_k(x_a^{ji}))] - \text{KL}[q(\mathbf{u}) \parallel p(\mathbf{u})]. \quad (6.6)$$

In all of the above we have purposefully omitted h_w , the neural net, from the notation.

7. EXPERIMENT: DKL INVARIANCE LEARNING WITH SOFTMAX LIKELIHOOD

7.1. Rotated MNIST. The rotated MNIST dataset² was generated from the original MNIST dataset by randomly rotating the images of hand-written digits between 0 and 2π radians. It consists of a training set of 12.000 images along with 50.000 such images for testing. We pretrain the neural network from Sec. 5.2 on rotated MNIST (Table 1, M1) and proceed as outlined in Sec. 5.1. As discussed in Sec 5.1, we do not have guarantees that the ELBO acts as a good model selector for the neural network hyperparameters. We thus use a validation set (3000 of the 12000 training points) to find hyperparameters for the weight updates. When a good

²https://sites.google.com/a/lisa.iro.umontreal.ca/public_static_twiki/variations-on-the-mnist-digits

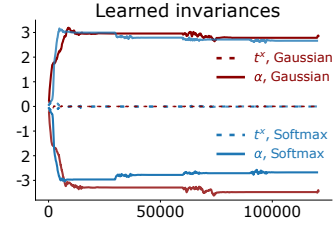


FIGURE 7. Learned invariance parameters (rotation α in radians and x-translation t_x) for rotMNIST. Note the different scaling of the y -axis to Fig. 6.

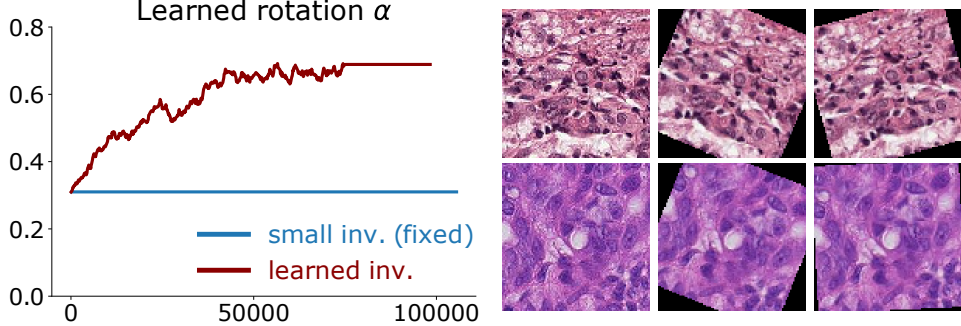


FIGURE 8. *Left*: Learned rotation on PCam. *Right*: PCam orbit samples. Augmented images look smoother due to interpolation, thus we preprocess the dataset with small rotations when learning invariances.

training setting is found we proceed with training on the entire training set (see Appendix for these settings). Fig. 7 shows the learned invariances (for brevity, we only illustrate rotation in radians and x -translation). Both Gaussian and Softmax models learn to be rotation-invariant close the full 2π rotations present in the data. Table 1 contains test accuracies. Deep kernel GPs outperform their shallow counterparts by large margins (differences in test accuracy of ≥ 10 percent points). The same is true for invariant compared to non-invariant models (≥ 3 percent points). While both likelihoods achieve similar test accuracies, we observe a $2.3\times$ speedup in training for the sample-based Softmax over the Gaussian model. Gaussian model: 2.64 seconds per iteration, Gaussian + sample bound: 1.32 sec./iter., Softmax + sample bound: 1.13 sec./iter. All runs are executed on 12 GB Nvidia Titan X/Xp GPUs.

7.2. PatchCamelyon. The PatchCamelyon (PCam, CC0 License, [Veeling et al., 2018]) dataset consists of histopathology scans of lymph nodes measuring $96 \times 96 \times 3$ pixels. Labels indicate whether the center patch contains at least one tumor pixel. Veeling et al. [2018] improve test set performance from 0.876 to 0.898 by using a model architecture which is invariant to (hard-coded) 90° rotations of the input. Such discrete, non-differentiable augmentations are not compatible with our backpropagation based method, so we instead work with continuously sampled rotations (i.e. a special case of the transformations described in Sec. 3.3 with $\phi = (\alpha)$ and $\alpha_{min} = -\alpha_{max}$). This, contrary to Veeling et al. [2018]’s approach, introduces the need for padding as well as interpolation (see Fig. 8, left), effectively changing the data distribution. We thus apply small rotations as a pre-processing step ($\pi/10$ radians, ‘small inv.’ in Table 2). This lowers performance for a CNN alone, i.e. when pre-training the weight hyperparameters. The invariant models counterbalance this performance drop, and the learned invariances produce the best results in our experiments, however, results remain subpar to Veeling et al. [2018]. This is due to the discussed limitation to differentiable image transformations, as well as the simpler model architecture employed in our experiment (see Appendix). We highlight that our task is fundamentally different in nature: instead of hard-coding invariances we *learn* those during optimisation.

Model	Test acc.
CNN	0.7905
Deep Kernel GP + no inv.	0.8018
CNN + small inv.	0.7420
Deep Kernel GP + small inv.	0.8115
Deep Kernel GP + learned inv.	0.8171

TABLE 2. PCam results. Deep Kernel GP model with learned inv. performs best.

8. CONCLUSION AND LIMITATIONS

Neural networks depend on good inductive biases in order to generalise well. Practitioners usually – successfully – hand craft such inductive biases, but the idea of learning such model properties from data is appealing: Might we automate the modelling pipeline, moving from hand-crafted models to data driven models; much like we replaced hand crafted features with learned features in deep neural networks? This work proposes one step in this direction. Inspired by theory on Bayesian model selection we employ the marginal likelihood as a loss function for learning inductive biases. We avoid the intractability of the marginal likelihood for neural networks by using Deep Kernel Learning, which also enables us to leverage previous work on invariance learning in GPs for learning data augmentation in neural networks. We learn useful invariances and improve performance on rotated MNIST and in the small data regime, but encounter challenges when optimising our models. Some of those challenges we address by introducing a new sampling-based bound to the ELBO which allows for inference for the Softmax likelihood (the natural choice for classification problems).

The key limitation of (invariant) DKL is that we only marginalise the last layer which leaves the neural network hyperparameters unmarginalised, and the ELBO can overfit these [Ober et al., 2021]. We believe that ongoing research in Bayesian Deep Learning will alleviate this problem with methods for marginalising over lower layers too, protecting them against overfitting. Another limitation is that we can currently only employ differentiable image transformation (see Sec. 7.2). This prevents us from learning popular augmentation schemes like flipping, but could be overcome by implementing score functions [Sutton et al., 1999].

Broader Impact: This work is situated within basic research in probabilistic ML and, as such, bears all the risks of automation itself: harmful redistribution of wealth to those with access to compute resources and data, loss of jobs, etc.. We comment here on two specific concerns. *Invariances and Fairness:* As seen in Sec. 5.2, our learned invariances can be leveraged to augment small datasets, resulting in significant performance improvements. We hope that this idea finds application in the context of fairness, where algorithmic bias often stems from under-representation, i.e. small samples from certain demographic groups. *Environmental impact:* Our model is significantly more computationally heavy than a standard neural network with hand-tuned data augmentation. However, in the long term, automatic model selection has the potential to *reduce* the need for hyperparameter tuning, which usually dramatically exceeds the resources needed for training the final model.

ACKNOWLEDGEMENTS

MJ was supported by a research grant (15334) from VILLUM FONDEN and the Carlsberg Foundation (CF20-0370). The majority of this work was done while MJ was affiliated with the Technical University of Denmark. SWO acknowledges the support of the Gates Cambridge Trust for his doctoral studies.

REFERENCES

G. Benton, M. Finzi, P. Izmailov, and A. G. Wilson. Learning invariances in neural networks. *arXiv preprint arXiv:2010.11882*, 2020.

C. Blundell, J. Cornebise, K. Kavukcuoglu, and D. Wierstra. Weight uncertainty in neural networks. In *International Conference on Machine Learning*. PMLR, 2015.

J. Bradshaw, A. G. d. G. Matthews, and Z. Ghahramani. Adversarial examples, uncertainty, and transfer testing robustness in gaussian process hybrid deep networks. *arXiv preprint arXiv:1707.02476*, 2017.

T. D. Bui, J. Yan, and R. E. Turner. A unifying framework for gaussian process pseudo-point approximations using power expectation propagation. *Journal of Machine Learning Research*, 18(104):1–72, 2017. URL <http://jmlr.org/papers/v18/16-603.html>.

D. R. Burt, C. E. Rasmussen, and M. van der Wilk. Convergence of sparse variational inference in gaussian processes regression. *Journal of Machine Learning Research*, 21(131):1–63, 2020. URL <http://jmlr.org/papers/v21/19-1015.html>.

R. Calandra, J. Peters, C. E. Rasmussen, and M. P. Deisenroth. Manifold gaussian processes for regression. In *2016 International Joint Conference on Neural Networks (IJCNN)*, pages 3338–3345. IEEE, 2016.

E. D. Cubuk, B. Zoph, D. Mane, V. Vasudevan, and Q. V. Le. Autoaugment: Learning augmentation strategies from data. In *Proceedings of the IEEE/CVF Conference on Computer Vision and Pattern Recognition*, pages 113–123, 2019.

E. D. Cubuk, B. Zoph, J. Shlens, and Q. V. Le. Randaugment: Practical automated data augmentation with a reduced search space. In *Proceedings of the IEEE/CVF Conference on Computer Vision and Pattern Recognition Workshops*, pages 702–703, 2020.

A. Damianou and N. D. Lawrence. Deep gaussian processes. In *Artificial intelligence and statistics*, pages 207–215. PMLR, 2013.

V. Dutordoir, M. Wilk, A. Artemev, and J. Hensman. Bayesian image classification with deep convolutional gaussian processes. In *International Conference on Artificial Intelligence and Statistics*, pages 1529–1539. PMLR, 2020.

V. Dutordoir, J. Hensman, M. van der Wilk, C. H. Ek, Z. Ghahramani, and N. Durrande. Deep neural networks as point estimates for deep gaussian processes, 2021.

S. Hauberg, O. Freifeld, A. B. L. Larsen, J. W. F. III, and L. K. Hansen. Dreaming more data: Class-dependent distributions over diffeomorphisms for learned data augmentation. In *Proceedings of the 19th international Conference on Artificial Intelligence and Statistics (AISTATS)*, volume 51, pages 342–350, 2016.

J. Hensman, N. Fusi, and N. D. Lawrence. Gaussian processes for big data. *arXiv preprint arXiv:1309.6835*, 2013.

G. E. Hinton and R. R. Salakhutdinov. Using deep belief nets to learn covariance kernels for gaussian processes. *Advances in neural information processing systems*, 20:1249–1256, 2007.

D. Ho, E. Liang, X. Chen, I. Stoica, and P. Abbeel. Population based augmentation: Efficient learning of augmentation policy schedules. In *International Conference on Machine Learning*, pages 2731–2741. PMLR, 2019.

A. Immer, M. Bauer, V. Fortuin, G. Rätsch, and M. E. Khan. Scalable marginal likelihood estimation for model selection in deep learning, 2021.

M. Jaderberg, K. Simonyan, A. Zisserman, and K. Kavukcuoglu. Spatial transformer networks. *arXiv preprint arXiv:1506.02025*, 2015.

Y. LeCun, C. Cortes, and C. Burges. Mnist handwritten digit database. *ATT Labs [Online]. Available: <http://yann.lecun.com/exdb/mnist>*, 2, 2010.

D. J. MacKay. *Model Comparison and Occam’s Razor*. Cambridge university press, 2002.

A. G. d. G. Matthews, J. Hensman, R. Turner, and Z. Ghahramani. On sparse variational methods and the kullback-leibler divergence between stochastic processes. In *Artificial Intelligence and Statistics*, pages 231–239. PMLR, 2016.

M. Minsky. Steps toward artificial intelligence. *Proceedings of the IRE*, 49(1):8–30, 1961.

S. W. Ober and L. Aitchison. Global inducing point variational posteriors for bayesian neural networks and deep gaussian processes. *arXiv preprint arXiv:2005.08140*, 2020.

S. W. Ober, C. E. Rasmussen, and M. van der Wilk. The promises and pitfalls of deep kernel learning. *arXiv preprint arXiv:2102.12108*, 2021.

C. E. Rasmussen and Z. Ghahramani. Occam’s razor. *Advances in neural information processing systems*, pages 294–300, 2001.

R. S. Sutton, D. A. McAllester, S. P. Singh, Y. Mansour, et al. Policy gradient methods for reinforcement learning with function approximation. In *NIPS*, volume 99, pages 1057–1063. Citeseer, 1999.

M. Titsias. Variational learning of inducing variables in sparse gaussian processes. In D. van Dyk and M. Welling, editors, *Proceedings of the Twelfth International Conference on Artificial Intelligence and Statistics*, volume 5 of *Proceedings of Machine Learning Research*, pages 567–574, Hilton Clearwater Beach Resort, Clearwater Beach, Florida USA, 16–18 Apr 2009. PMLR. URL <http://proceedings.mlr.press/v5/titsias09a.html>.

R. E. Turner and M. Sahani. Two problems with variational expectation maximisation for time-series models. In D. Barber, T. Cemgil, and S. Chiappa, editors, *Bayesian Time series models*, chapter 5, pages 109–130. Cambridge University Press, 2011.

M. van der Wilk, M. Bauer, S. John, and J. Hensman. Learning invariances using the marginal likelihood. In *Advances in Neural Information Processing Systems*, pages 9938–9948, 2018.

M. van der Wilk, V. Dutordoir, S. John, A. Artemev, V. Adam, and J. Hensman. A framework for interdomain and multioutput gaussian processes, 2020.

B. S. Veeling, J. Linmans, J. Winkens, T. Cohen, and M. Welling. Rotation equivariant CNNs for digital pathology. In *International Conference on Medical image computing and computer-assisted intervention*, pages 210–218. Springer, 2018.

C. K. Williams and C. E. Rasmussen. *Gaussian processes for machine learning*. MIT press Cambridge, MA, 2006.

A. G. Wilson, Z. Hu, R. Salakhutdinov, and E. P. Xing. Deep kernel learning. In *Artificial intelligence and statistics*, pages 370–378, 2016a.

A. G. Wilson, Z. Hu, R. R. Salakhutdinov, and E. P. Xing. Stochastic variational deep kernel learning. *Advances in Neural Information Processing Systems*, 29: 2586–2594, 2016b.

J. T. Wilson, V. Borovitskiy, A. Terenin, P. Mostowsky, and M. P. Deisenroth. Efficiently sampling functions from gaussian process posteriors. *arXiv preprint arXiv:2002.09309*, 2020.

APPENDIX A. EXPERIMENT DETAILS

A.1. MNIST variations. For reproducibility, we here summarise the training setups for the experiments on MNIST variations, i.e. MNIST subsets (Section 5.2) and rotated MNIST (Section 7.1). We start by outlining the shared neural network architecture and will then list the hyperparameter settings for MNIST and rotMNIST, respectively.

The CNN architecture used in the (rot)MNIST experiments is depicted in Table 3. For rotated MNIST, we train the model for 200 epochs with the Adam optimiser (default parameters). For the MNIST subsets, we train for 60k iterations which corresponds to 200 epochs for the full dataset and respectively more epochs for smaller subsets. The remaining parameters are the same in all experiments: batch size 200, learning rate 0.001, no weight decay, other regularisation or data augmentation. In the pre-training phase we minimise negative log-likelihood, for updates during coordinate ascent we use the ELBO as a loss-function.

Layer	Specifications
Convolution	filters=20, kernel size=(5, 5), padding=same, activation=ReLU
Max pooling	pool size=(2, 2), stride=2
Convolution	filters=50, kernel size=(5, 5), padding=same, activation=ReLU
Max pooling	pool size=(2, 2), stride=2
Fully connected	neurons=500, activation=ReLU
Fully connected	neurons=50, activation=ReLU
Fully connected	neurons=10, activation=Softmax

TABLE 3. Neural network architecture for MNIST variations. After pre-training, the last fully connected layer (below dashed line) is replaced with a GP layer for the deep kernel models.

Hyperparameter initialisation for the MNIST subset experiments. are lengthscale 10, likelihood variance 0.05, kernel variance 1 (fixed likelihood and kernel variance for the invariant model, see Sec. 5.2), posterior variance 0.01. We use 1200 inducing points which we initialise by first passing the images through the neural network, then using the ‘greedy variance’ method [Burt et al., 2020] on the extracted features. For the smallest dataset MNIST312 we use 312 inducing points only. The batch size is 200 and we choose learning rate 0.001 for the Adam optimiser. For the invariant models, the orbit size is 120 and affine parameters are initialised at $\phi_{min} = \phi_{max} = 0.02$, i.e. we initialise with a small invariance. Without this initialisation we encountered occasional numerical instabilities (Cholesky errors) on the small dataset runs. During coordinate ascent (InvDKGP models) we toggle between training GP and CNN after 25k steps.

Hyperparameter initialisation for the rotMNIST experiment. as follows: For all models, we initialise kernel variance 1 (fixed at 1 for M9, see Sec. 5.2) and posterior variance 0.01. We use 1200 inducing points. For the invariant models, the orbit size is 120 and affine parameters are initialised at $\phi_{min} = \phi_{max} = 0$, i.e. invariances are learned from scratch. When using coordinate ascent (InvDKGP models, M8 & M9) we toggle between training GP and CNN after 30k steps. We train different models for a different number of iterations, all until the ELBO has roughly converged. Batch size 200 is used for all models. The remaining initialisations differ between models and are summarised in Table 4.

	Model	Lengthsc.	Lik. var.	LR (decay)
M2	Non-inv. Shallow GP + Gaussian	10	0.02	0.001
M3	Non-inv. Shallow. GP + Softmax	10	-	0.001
M4	Inv. Shallow GP + Gaussian	10	0.05	0.001
M5	Inv. Shallow. GP + Softmax	10	-	0.001
M6	Non-inv. Deep Kernel GP + Gaussian	10	0.05	0.001
M7	Non-inv. Deep Kernel GP + Softmax	20	-	0.001
M8	Inv. Deep Kernel GP + Gaussian	50	0.05 (F)	0.003 (steps / cyclic)
M9	Inv. Deep Kernel GP + Softmax	9	-	0.003 / 0.0003 (s / c)

TABLE 4. Training settings for rotMNIST models: Kernel lengthscale and likelihood variance initialisations ('F' indicates a fixed likelihood variance, see Sec. 5.2). The learning rate column ('LR') also indicates whether the learning rate was decayed in the GP/CNN update phases of coordinate ascent. For the 'steps'(s) decay, we divide by 10 after 50% and again 75% of iterations, for the 'cyclic'(c) decay, learning rates are: [LR/100, LR/10, LR, LR/10, LR/100]. These training hyperparameters are determined using a validation set (see Sec. 7.1).

A.2. PCam.

The CNN architecture. is a VGG-like convolutional neural network³ described in Table 5. The model is trained for 5 epochs using the Adam optimiser with batch size 64. We use learning rate 0.001 which we divide by 10 after 50% and again 75% of training iterations. In the fully connected block we use dropout with 50% probability when pre-training. Dropout is disabled when training the deep kernel models.

Layer	Specifications
Convolution	filters=16, kernel size=(3, 3), padding=valid, activation=ReLU
Convolution	filters=16, kernel size=(3, 3), padding=valid, activation=ReLU
Max Pooling	pool size=(2, 2), strides=2
Convolution	filters=32, kernel size=(3, 3), padding=valid, activation=ReLU
Convolution	filters=32, kernel size=(3, 3), padding=valid, activation=ReLU
Max Pooling	pool size=(2, 2), stride=2
Convolution	filters=64, kernel size=(3, 3), padding=valid, activation=ReLU
Convolution	filters=64, kernel size=(3, 3), padding=valid, activation=ReLU
Max Pooling	pool size=(2, 2), stride=2
Fully Connected	neurons=256, activation=ReLU
Dropout	probability=0.5
Fully Connected	neurons=50, activation=None
Dropout	probability=0.5
Fully connected	neurons=2, activation=Softmax

TABLE 5. Neural network architecture for PCAM. After pre-training, the last fully connected layer (below dashed line) is replaced with a GP layer for the deep kernel models and dropout is disabled.

Hyperparameters. for the deep kernel GP experiments on PCam are: lengthscales 10 (1 for the learned invariance model), kernel variance 1, posterior variance 0.01. We use 750 inducing points which we initialise as in the previous experiments. The

³We closely follow <https://geertlitjens.nl/post/getting-started-with-camelyon/>.

batch size is 32. For PCAm we use coordinate ascent for all models since this improves training stability. Learning rates are 0.001 for the GP update steps and 0.0001 for the CNN updates, no LR decay. We toggle between the two coordinate ascent phases after 50k and 75k iterations in the non-invariant and invariant case, respectively. For the invariant models the orbit size is 20 and we initialise the rotation invariance with $\phi_{min/max} = \alpha_{min/max} = \pm\pi/10$.